LETTER *Earth Planets Space*, **60**, 117–122, 2008

Magnetotelluric observations around the focal region of the 2007 Noto Hanto Earthquake (M_j 6.9), Central Japan

Ryokei Yoshimura[1], Naoto Oshiman[1], Makoto Uyeshima[2], Yasuo Ogawa[3], Masaaki Mishina[4], Hiroaki Toh[5], Shin'ya Sakanaka[6], Hiroshi Ichihara[7], Ichiro Shiozaki[8], Tsutomu Ogawa[2], Tsutomu Miura[1], Shigeru Koyama[2], Yasuyoshi Fujita[1], Kazuhiro Nishimura[1], Yu Takagi[1], Mikihiro Imai[6], Ryo Honda[7], Sei Yabe[1], Shintaro Nagaoka[3], Mitsuhiro Tada[1], and Toru Mogi[7]

[1]*Disaster Prevention Research Institute, Kyoto University, Japan*
[2]*Earthquake Research Institute, University of Tokyo, Japan*
[3]*Volcanic Fluid Research Center, Tokyo Institute of Technology, Japan*
[4]*Research Center for Prediction of Earthquakes and Volcanic Eruptions, Tohoku University, Japan*
[5]*Department of Earth Sciences, University of Toyama, Japan*
[6]*Department of Earth Science and Technology, Akita University, Japan*
[7]*Institute of Seismology and Volcanology, Hokkaido University, Japan*
[8]*Department of Civil Engineering, Tottori University, Japan*

(Received June 30, 2007; Revised September 3, 2007; Accepted September 10, 2007; Online published February 19, 2008)

On 25 March 2007, a damaging earthquake (M_j 6.9) occurred near the west coast of the Noto Peninsula, Central Japan. A wideband magnetotelluric (MT) survey was carried out in the onshore area of the source region immediately after the mainshock, with the aim of imaging the heterogeneity of the crustal resistivity structure. The final observation network had consisted of 26 sites. As a preparatory step for imaging three-dimensional features of the resistivity around the focal region, we constructed two-dimensional resistivity models along five profiles using only the TM mode responses, in order to reduce three-dimensional effects. Four profiles are perpendicular to the fault strike, and a fifth profile is parallel to the strike through the mainshock epicenter. Significant characteristics of the resistivity models are: (1) beneath the mainshock hypocenter, there is a conductive body which spreads to the eastern edge of the active aftershock region; (2) a resistive zone is located in the gap of the aftershock distribution between the mainshock hypocenter and the largest eastern aftershock; (3) one of the largest aftershock occurred at the boundary of the resistive zone described above. These results suggest that the deep conductors represent fluid-filled zones and that the lateral heterogeneity could have controlled the slip distribution on the fault plane.
Key words: Resistivity structure, wideband magnetotellurics, 2007 Noto Hanto Earthquake.

1. Introduction

The 2007 Noto Hanto Earthquake, M_j 6.9 determined by the Japan Meteorological Agency (JMA), occurred at 09:42 (JST) on 25 March 2007 near the west coast of the Noto Peninsula (Noto Hanto) which is located in the back arc area of Central Japan (Fig. 1). According to a preliminary moment tensor solution of the National Research Institute for Earth Science and Disaster Prevention (NIED, 2007), this earthquake has a compressional axis in a WNW–ESE direction, and the focal mechanism shows a reverse fault with a small amount of strike-slip component. The faulting geometry was also estimated from a Global Positioning System (GPS) analysis by the Geographical Survey Institute (GSI, 2007) as a reverse fault type with a strike of approximately N55°E and a dip of approximately 63°. A previous large earthquake, which occurred about 10 km off the northeastern tip of the Noto Peninsula in 1993 (M_j 6.6), also occurred on a reverse fault (e.g. Ito *et al.*, 1994), similar to the earthquake in 2007.

The two largest aftershocks, both M_j 5.3, occurred at 18:11 on 25 March near the northeastern edge of the aftershock region and at 07:16 on 26 March near the southwestern edge. JMA (2007) reported that there are gaps in the aftershock distribution between the mainshock hypocenter and the two largest aftershocks. Also, the two largest aftershocks occurred at places where stress had accumulated due to the mainshock, based on a variation of the Coulomb Failure Function (ΔCFF) analysis.

We performed a wideband magnetotelluric (MT) survey immediately after the occurrence of the mainshock with the aim of showing along-strike variations of the structure—i.e. differences between the mainshock hypocentral region, the gap in the aftershock distribution, and the region of the eastern largest aftershock. Electromagnetic investigations have recently played an important role in grasping properties around seismogenic regions of not only plate-boundary (e.g. Unsworth *et al.*, 2000; Ogawa and Honkura, 2004; Tank *et al.*, 2005) but also intraplate earthquakes (e.g. Mitsuhata *et al.*, 2001; Ogawa *et al.*, 2001; Uyeshima *et al.*, 2005). In view of the sensitivity of resistivity to the ex-

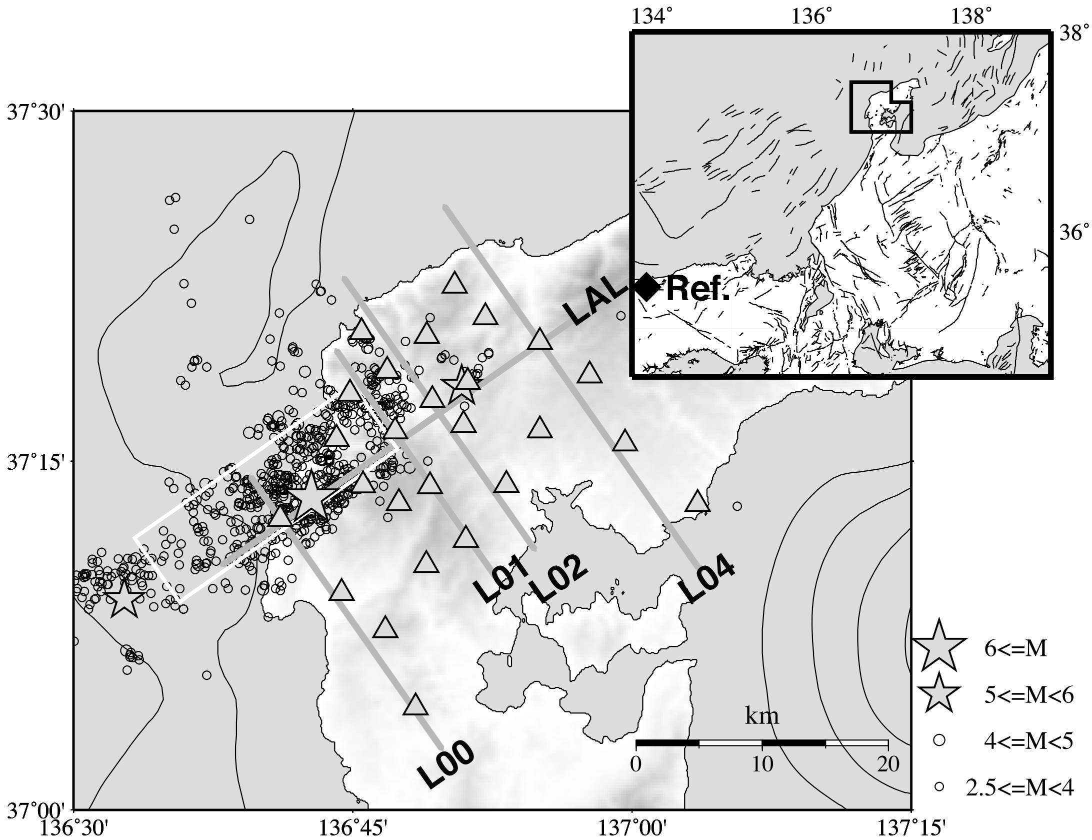

Fig. 1. Magnetotelluric (MT) site locations are shown by gray triangles. The epicenters of the mainshock and the two largest aftershocks are indicated by gray stars, have been relocated by Sakai *et al.* (2008). The other aftershocks determined by JMA are plotted as open circles. The fault plane estimated from a GPS analysis (GSI, 2007) is represented as a white rectangle. Two-dimensional inversions of the MT data were carried out for the thick gray lines labeled with the profile ID. Contours in the sea represent the water depth with intervals of 100 m (GINA global grid; Lindquist *et al.*, 2004). An index map is shown at the top right with active faults around Central Japan. A black diamond indicates a far-remote reference site.

istence of fluids, joint interpretations of electric properties with other geophysical information will extend our knowledge of the field conditions around source regions of intraplate earthquakes.

2. Data Acquisition and Inversions

2.1 MT measurements

To reveal the subsurface electrical resistivity structure, we carried out MT measurements (320 to 5×10^{-4} Hz) at 26 sites around the focal region of the 2007 Noto Hanto earthquake. A location map of the MT sites is shown in Fig. 1. The MT data were recorded from 4 April to 1 May 2007. We used up to 17 units of a five-component (three magnetic and two telluric channels) wideband MT system (MTU5/5A Phoenix Geophysics Ltd.) and two units of a two-component (two telluric channels) system (MTU2E Phoenix Geophysics Ltd.). The instruments were synchronized via signals from GPS satellites. In order to use the remote reference technique for reducing artificial local magnetic noise (Gamble *et al.*, 1979), we also acquired magnetic field data with the same type of instrument in central Tottori Prefecture, about 350 km southwest of the study area (Fig. 1). We calculated MT impedances using data only during 00:00–05:00 (JST) for each day to avoid electrical noise, especially the noise due to the leakage currents from DC electric railways. For the telluric-only sites (six of 26 sites), magnetic field data were taken from nearby sites with good-quality data to calculate impedances. The different locations of the telluric and magnetic fields measurements were taken into consideration in the two-dimensional inversions.

2.2 Two-dimensional inversions

As a preparatory step for imaging three-dimensional features of resistivity around the focal region, we constructed two-dimensional resistivity models along five profiles using only the TM mode responses. Previous studies (e.g. Wannamaker *et al.*, 1984; Wannamaker, 1999; Ogawa, 2002; Siripunvaraporn *et al.*, 2005) have shown that TM mode data are least affected by three-dimensional effects. Four profiles (L00, L01, L02 and L04 in Fig. 1) are perpendicular to the fault strike, and the fifth (LAL in Fig. 1) is parallel to the strike through the mainshock epicenter. To implement the two-dimensional inversions, we rotated the impedance tensors (55° and −35° for profiles perpendicular and parallel to the fault strike, respectively) and classified their off-diagonal terms into TM and TE modes. The electric field is parallel to the two-dimensional profile for the TM mode. Figure 2 shows the five resistivity models following the two-dimensional inversions using the code of Ogawa and Uchida (1996). In the inversions, the error floor values for the apparent resistivity were set at 5%, and equivalent values were set for the phase. The root mean square (RMS) values of the five profiles were 0.64 (L00), 0.78 (L01), 0.69 (L02), 0.89 (L04), and 0.90 (LAL). The resistivity struc-

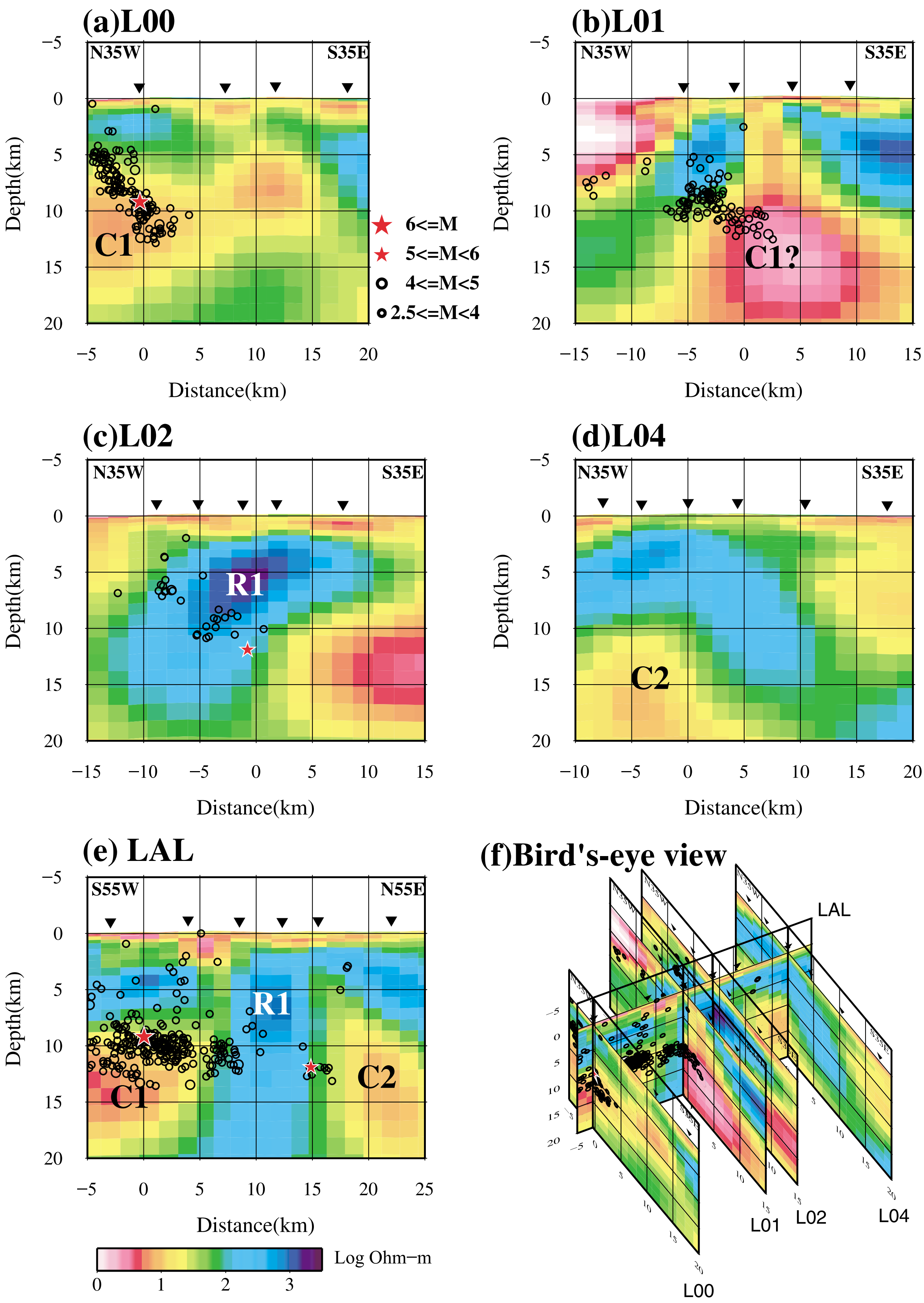

Fig. 2. Obtained resistivity models of the profiles; (a) L00, (b) L01, (c) L02, (d) L04 and (e) LAL, which are represented in Fig. 1. (f) Bird's-eye view of all profiles from the southern direction. Inverted triangles indicate the locations of the MT sites. The mainshock and the largest aftershock are shown as red stars, and other aftershocks in a 4-km wide swath are plotted as open circles on each profile. Features labeled C1, C2, and R1 are discussed in the text.

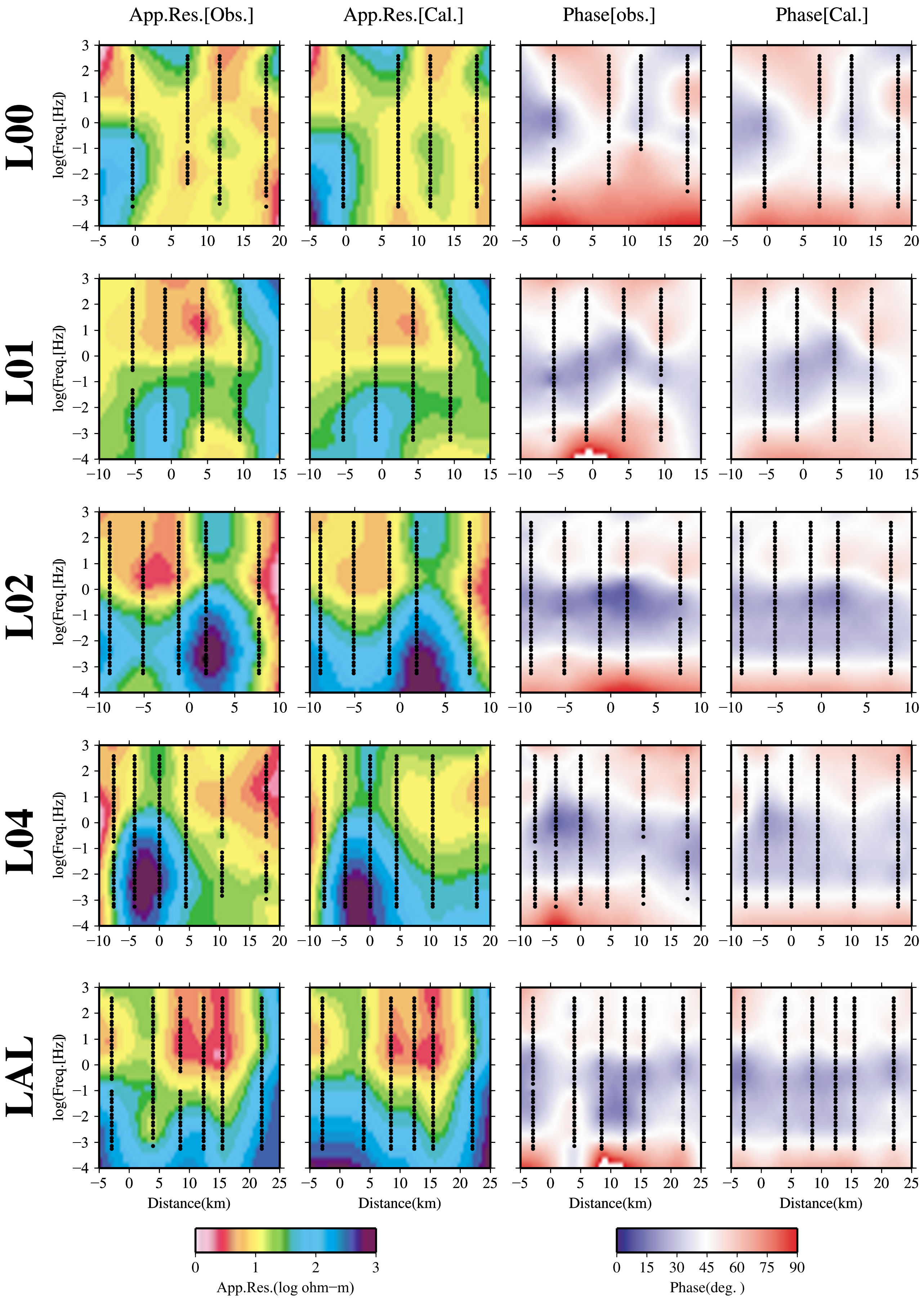

Fig. 3. Pseudo-sections for the observed and calculated data. Rows 1 to 5 show the profiles L00, L01, L02, L04 and LAL, respectively. Columns 1–4 are the observed and calculated apparent resistivity, and the observed and calculated phase for the TM mode, respectively.

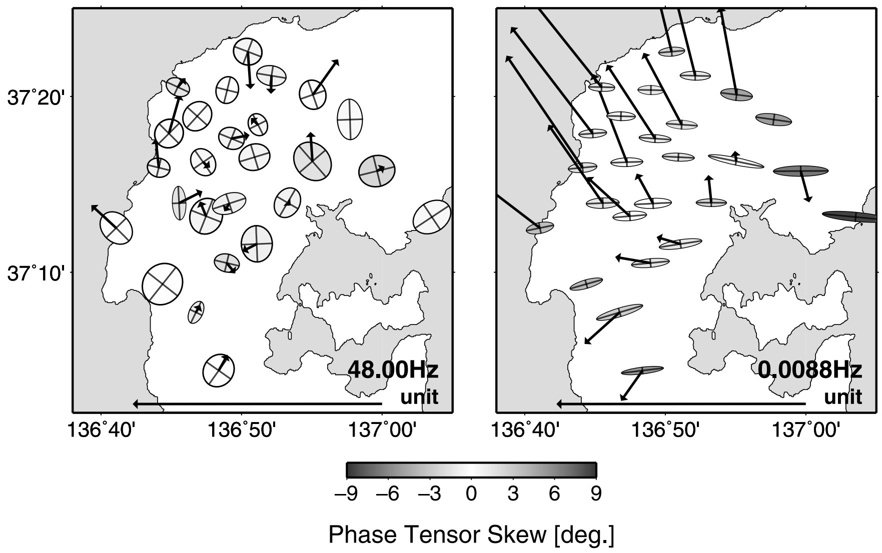

Fig. 4. Spatial distribution of the real induction vectors (black arrows) and the phase tensor ellipses for 48 (left) and 0.0088 (right) Hz. The induction vectors point towards zones of conductors. Phase tensor ellipses (Caldwell *et al.*, 2004) are shown with their principal axes. Gray scale indicates the skew angle of the phase tensor. The phase tensor is unaffected by a galvanic distortion of the electric field and its skew angle indicates the asymmetry of the phase response produced by the three-dimensional structure. In the case of the two-dimensional electrical structure, the ellipses will be oriented either parallel or perpendicular to the electrical strike of the structure.

ture of the Sea of Japan, which surrounds our study area, was included in the inversions by specifying the bathymetry along the two-dimensional profiles and a resistivity of sea water as 0.25 Ω m. In each inversion, a uniform earth of 100 Ω m, including the topography, was used as the initial model. Figure 3 shows comparisons between the observed and calculated data for each profile.

The results show a good general agreement between the four profiles across the fault strike and the profile along the strike. These models exhibit two significant features. The first observation is that there are two conductive blocks at a depth greater than 10 km, one near the lower part of the fault (C1) and the other in the region of an eastward extension of the fault (C2). The other observation is that there is a resistive zone (R1), which extends from near the surface to greater depth, around the eastern edge of the fault. Although the configurations of the blocks are slightly uncertain because of the three-dimensional effects, the data are found to be sufficiently sensitive to the main features of the model.

3. Discussion and Conclusions

The hypocenter of the 2007 Noto Hanto Earthquake is located above a conductive block (C1), and the aftershocks associated with the mainshock are also distributed along the top surface of this conductor. Recent results of other MT surveys that image regions of intraplate earthquakes (e.g. Mitsuhata *et al.*, 2001; Ogawa *et al.*, 2001; Uyeshima *et al.*, 2005) show that seismogenic regions of intraplate earthquakes are located near boundaries between resistive and conductive blocks. There are several possible candidates for explaining the existence of conductors within the Earth's crust and upper mantle, including fluids, partial melting, and high temperature. In our study area, it is difficult to consider the latter two possibilities as explaining the existence of the conductor because of the distance from the volcanic front. Kato *et al.* (2008) elucidated a detailed velocity structure by using data from a dense temporal seismic network and detected a distinct low velocity anomaly near and beneath the mainshock that corresponds to the C1 block. This correlation between the seismic tomography and magnetotelluric images may suggest that the conductor represents a fluid-filled zone. However, the MT observation sites do not cover the whole region of the earthquake because the southwestern half of the fault is located under the sea, as shown in Fig. 1. In order to confirm the whole image of the conductor, we expect to perform several ocean bottom magnetotelluric measurements.

We also find that eastern part of the conductor (C1) seems to spread toward the edge of the active aftershock region, and the resistive zone (R1) appears to block the eastward broadening of the conductor. In addition, this resistive zone is located in the gap of the aftershock distribution between the mainshock hypocenter and the largest eastern aftershock. The good correlation between the absence of aftershocks and the location of R1 implies that the heterogeneities of the lateral structure could have controlled the slip distribution on the fault plane. The largest aftershock occurred near the boundary between R1 and C2. JMA (2007) pointed that stress is accumulated from the mainshock in this region. Accordingly, it is suggested that the resistive zone (R1) may be interpreted as a segment that remains locked.

Figure 4 shows the spatial distribution of the induction vectors (IV) and the phase tensor (PT) ellipses (Caldwell *et al.*, 2004) for 48 and 0.0088 Hz. Although the IV and PT ellipses for the higher frequency, which represent the shallow region, comprehensively support the results of our inversions, the distributions of the IV and PT show an essentially three-dimensional situation. On the other hand, the distributions for the lower frequency, which represent the deep region, strongly indicate a two-dimensional structure.

The IV and PT results suggest that the study area is under the situation of three-dimensional/two-dimensional. From this point, we will expand our study to a three-dimensional analysis including the complete data set in order to reveal the detailed features of the electrical structure around the focal region.

Acknowledgments. We would like to express our sincere appreciation to the landowners who kindly permitted us to use their properties to make measurements despite severe conditions just after the earthquake disaster. S. Sakai provided hypocenter data of the mainshock and largest aftershocks. Other seismic data were provided by the Japan Meteorological Agency. Valuable comments from S. B. Tank and another anonymous reviewer helped us in improving the manuscript. We are also grateful to J. Mori for helpful comments on this paper. This work was funded by 'The 2nd new Program of Research and Observation for Earthquake Prediction' of the Ministry of Education, Culture, Sports, Science and Technology of Japan (MEXT) and a Grant-in-Aid for Special Purposes (19900001) offered from MEXT. This work was also supported by the Earthquake Research Institute cooperative research program (2007-A-07). Several figures were prepared with the GMT provided by Wessel and Smith (1998).

References

Caldwell, T. G., H. M. Bibby, and C. Brown, The magnetotelluric phase tensor, *Geophys. J. Int.*, **158**, 457–469, 2004.

Gamble, T. D., W. M. Goubau, and J. Clarke, Magnetotellurics with a remote magnetic reference, *Geophysics*, **44**, 53–67, 1979.

Geographical Survey Institute (GSI), Crustal Movements in the Hokuriku and Chubu District, *Report of The Coordinating Committee for Earthquake Prediction*, **78**, 424–456, 2007 (in Japanese).

Ito, K., H. Wada, K. Watanabe, H. Horikawa, T. Tsukuda, and K. Sakai, 1993 off Noto Peninsula earthquake, *Annuals. Disas. Prev. Res. Inst., Kyoto Univ.*, **37**, 325–341, 1994 (in Japanese with English abstract).

Japan Meteorological Agency (JMA), The Noto Hanto earthquake in 2007, *Report of The Coordinating Committee for Earthquake Prediction*, **78**, 346–370, 2007 (in Japanese).

Kato, A., S. Sakai, T. Iidaka, T. Iwasaki, E. Kurashimo, T. Igarashi, N. Hirata, T. Kanazawa, and Group for the aftershock observations of the 2007 Noto Hanto Earthquake, Three-dimensional velocity structure in the source region of the Noto Hanto Earthquake in 2007 imaged by a dense seismic observation, *Earth Planets Space*, **60**, this issue, 105–110, 2008.

Lindquist, K. G., K. Engle, D. Stahlke, and E. Price, Global topography and bathymetry grid improves research efforts, *Eos Trans. AGU*, **85**(19), 186, 2004.

Mitsuhata, Y., Y. Ogawa, M. Mishina, T. Kono, T. Yokokura, and T. Uchida, Electromagnetic heterogeneity of the seismogenic region of 1962 M6.5 Northern Miyagi Earthquake, northeastern Japan, *Geophys. Res. Lett.*, **28**(23), 4371–4374, 2001.

National Research Institute for Earth Science and Disaster Prevention (NIED), Seismic activity of the 2007 Noto Peninsula earthquake (Mj6.9), *Report of The Coordinating Committee for Earthquake Prediction*, **78**, 371–373, 2007 (in Japanese).

Ogawa, Y., On two-dimensional modeling of magnetotelluric field data, *Surveys Geophys.*, **23**, 251–273, 2002.

Ogawa, Y. and Y. Honkura, Mid-crustal electrical conductors and their correlations to seismicity and deformation at Itoigawa-Shizuoka Tectonic Line, *Earth Planets Space*, **56**, 1285–1291, 2004.

Ogawa, Y. and T. Uchida, A two-dimensional magnetotelluric inversion assuming Gaussian static shift, *Geophys. J. Int.*, **126**, 69–76, 1996.

Ogawa, Y., M. Mishina, T. Goto, H. Satoh, N. Oshiman, T. Kasaya, Y. Takahashi, T. Nishitani, S. Sakanaka, M. Uyeshima, Y. Takahashi, Y. Honkura, and M. Matsushima, Magnetotelluric imaging of fluids in intraplate earthquake zones, NE Japan back arc, *Geophys. Res. Lett.*, **28**, 3741–3744, 2001.

Sakai, S., A. Kato, T. Iidaka, T. Iwasaki, E. Kurashimo, T. Igarashi, N. Hirata, T. Kanazawa, and the group for the joint aftershock observation of the 2007 Noto Hanto Earthquake, Highly-resolved distribution of aftershocks of the 2007 Noto Hanto Earthquake by a dense seismic observation, *Earth Planets Space*, **60**, this issue, 83–88, 2008.

Siripunvaraporn, W., G. Egbert, and M. Uyeshima, Interpretation of two-dimensional magnetotelluric profile data with three-dimensional inversion: synthetic examples, *Geophys. J. Int.*, **160**, 804–814, 2005.

Tank, S. B., Y. Honkura, Y. Ogawa, M. Matsushima, N. Oshiman, M. K. Tuncer, C. Celik, E. Tolak, and A. M. Isikara, Magnetotelluric imaging of the fault rupture area of the 1999 Izmit (Turkey) earthquake, *Phys. Earth Planet. Inter.*, **150**, 213–225, 2005.

Unsworth, M., P. Bedrosian, M. Eisel, G. Egbert, and W. Siripunvaraporn, Along strike variations in the electrical structure of the San Andreas Fault at Parkfield, California, *Geophys. Res. Lett.*, **27**(18), 3021–3024, 2000.

Uyeshima, M., Y. Ogawa, Y. Honkura, S. Koyama, N. Ujihara, T. Mogi, Y. Yamaya, M. Harada, S. Yamaguchi, I. Shiozaki, T. Noguchi, Y. Kuwaba, Y. Tanaka, Y. Mochido, N. Manabe, M. Nishihara, M. Saka, and M. Serizawa, Resistivity imaging across the source region of the 2004 Mid-Niigata Prefecture earthquake (M6.8), Central Japan, *Earth Planets Space*, **57**, 441–446, 2005.

Wannamaker, P. E., Affordable Magnetotellurics: Interpretation in Natural Environments, in *Three-dimensional electromagnetics*, edited by M. Oristaglio and B. Spies, 709 pp, Soc. Expl. Geophys, Tuls, 1999.

Wannamaker, P. E., G. W. Hohmann, and S. H. Ward, Magnetotelluric responses of three-dimensional bodies in layered earths, *Geophysics*, **49**, 1517–1533, 1984.

Wessel, P. and W. H. F. Smith, New, improved version of Generic Mapping Tools released, *EOS Trans. AGU*, **79**(47), 579, 1998.

R. Yoshimura (e-mail: ryokei@eqh.dpri.kyoto-u.ac.jp), N. Oshiman, M. Uyeshima, Y. Ogawa, M. Mishina, H. Toh, S. Sakanaka, H. Ichihara, I. Shiozaki, T. Ogawa, T. Miura, S. Koyama, Y. Fujita, K. Nishimura, Y. Takagi, M. Imai, R. Honda, S. Yabe, S. Nagaoka, M. Tada, and T. Mogi